Available online at www.sciencedirect.com
SCIENCE DIRECT®
International Journal of Pharmaceutics 271 (2004) 257–267
international journal of pharmaceutics
www.elsevier.com/locate/ijpharm

Influence of chitosan and its glutamate and hydrochloride salts on naproxen dissolution rate and permeation across Caco-2 cells

F. Maestrelli [a,*], N. Zerrouk [b], C. Chemtob [b], P. Mura [a]

[a] *Dipartimento di Scienze Farmaceutiche, Facoltà di Farmacia, Polo Scientifico di Sesto Fiorentino, Università di Firenze, Via U. Schiff 6, 50019 sesto Fiorentino, Firenze, Italy*

[b] *Laboratoire de Pharmacie Galénique, Faculté de Sciences Pharmaceutiques et Biologiques, Université de Paris V, 4 Avenue de l'Observatoire, 75270 Paris Cedex 06, France*

Received 23 May 2003; received in revised form 12 November 2003; accepted 19 November 2003

Abstract

Chitosan and its glutamate and hydrochloride salts were evaluated for their efficacy in improving the dissolution behaviour of naproxen (a poorly water-soluble antiinflammatory drug) and its transport in vitro across Caco-2 cell monolayers. Drug–polymer physical mixtures and coground products, prepared at two different w/w ratios (30/70 and 10/90), were characterized by differential scanning calorimetry, X-ray powder diffractometry, scanning electron microscopy, and tested for dissolution properties. Coground systems were more effective than physical mixtures in improving drug dissolution and chitosan base, in spite of its lower water solubility, showed higher solubilizing power than its salts. According to the solid state analyses results, this effect was directly related to its stronger amorphizing power. Transport studies showed that only coground mixtures with chitosan glutamate salt allowed a significant drug apparent permeability improvement; however, they did not exhibit appreciable effects on the Caco-2 tight junctions (measured by the trans-epithelial electrical resistance variations), thus indicating that their enhancer effect was mainly due to an improved naproxen transport by transcellular passive diffusion rather than through the paracellular route. The direct compression properties and antiulcerogenic activity together with the demonstrated dissolution and permeation enhancer abilities toward naproxen make chitosan glutamate an optimal carrier for developing fast-action oral solid dosage forms of this drug.

Keywords: Naproxen; Chitosan; Chitosan salts; Dissolution; Enhancer effect; Caco-2 cells

1. Introduction

According to the Amidon's biopharmaceutical classification system, dissolution in gastrointestinal fluids and permeability through biological membranes are the key parameters in bioavailability of orally administered drugs (Amidon et al., 1995).

Naproxen is a non-steroidal anti-inflammatory drug whose poor water solubility (0.025 mg/ml at 25 °C) and low dissolution rate are the limiting steps for its absorption (Amidon et al., 1995), potentially causing pharmacokinetic problems that decrease its clinical efficacy and increase the appearance of side-effects (Niazi et al., 1996). Chitosan is a natural-origin cationic polysaccharide obtained by *N*-deacetylation of chitin, resulting in a copolymer of *N*-acetyl-D-glucosamine and D-glucosamine (Illum, 1998). It is presently in development as a safe

* Corresponding author. Tel.: +39-055-4573672; fax: +39-055-4573671.
E-mail address: francesca.maestrelli@unifi.it (F. Maestrelli).

0378-5173/$ – see front matter © 2003 Elsevier B.V. All rights reserved.
doi:10.1016/j.ijpharm.2003.11.024

excipient in drug formulations (Baldrick, 2000) and it has found a number of applications in several drug delivery systems, in virtue of its high biocompatibility, biodegradability and lack of toxicity associated with gel- and film-forming abilities, bioadhesiveness, dissolution and transmucosal penetration enhancer properties (Illum, 1998; Paul and Sharma, 2000; Portero et al., 1998). Furthermore, its antiacid and antiulcer activities can be exploited to reduce gastric irritation caused by active compounds, such as anti-inflammatory drugs (Açikgoz et al., 1995).

We have recently demonstrated the effectiveness of chitosan in increasing the dissolution properties of naproxen (Mura et al., 2003). Moreover, in vivo studies on mice pointed out the efficacy of chitosan in promoting drug analgesic effect, thus suggesting a specific absorption enhancer effect of this polymer towards naproxen (Zerrouk et al., 2004).

Therefore, in the present study we thought it worthy of interest to extend our studies in order to elucidate the enhancer mechanism of chitosan towards naproxen and, furthermore, to compare its dissolution and enhancer properties with those of its more soluble salts, i.e. glutamate and hydrochloride, both examined at two different molecular weights.

Caco-2 cells, a colon rectal adenocarcinoma cell line of human origin were selected as the in vitro model for studying drug intestinal transport, since they have shown to be a valuable tool to investigate human intestinal absorption of drugs (Artursson, 1991; Lennernäs et al., 1996). Moreover, the effectiveness of Caco-2 cells in evaluating the transport enhancer properties of chitosan has been widely demonstrated (Artursson et al., 1994; Kotzé et al., 1997; Schipper et al., 1999; Dodane et al., 1999).

2. Materials and methods

2.1. Materials

Naproxen (NAP) (pK_a 4.5) and chitosan base (CS) (M_w 150 kDa) were supplied by Sigma (St. Louis, MO, USA). Chitosan hydrochloride (CSCl, Seacure® Cl113 (M_w 110 kDa) and Cl213 (M_w 272 kDa)) and glutamate (CSG, Seacure® G113 (M_w 128 kDa) and G213 (M_w 260 kDa)) were supplied by Pronova Biopolymer (Drammen, Norway). According to the relevant certificates of analysis, the degree of deacetylation was 87% for CSCl113, 84% for CSCl213, 85% for CSG113, 86% for CSG213 and 75–85% for CS. Solvents used in HPLC procedure were of HPLC grade. All other reagents were of analytical grade.

2.2. Preparation of solid systems

NAP–polymer solid systems at two different w/w ratios (30/70 and 10/90) have been prepared from the previously sieved (75–150 μm) individual components by: (a) physical mixing for 15 min in a turbula mixer; (b) cogrinding physical mixtures in a high-energy vibrational micromill for 60 min at 24 Hz.

2.3. Differential scanning calorimetry

DSC analysis was performed with a Mettler TA4000 apparatus equipped with a DSC 25 cell on 5–10 mg samples (Mettler M3 microbalance) scanned in pierced Al pans at 10 °C/min between 30 and 200 °C under static air.

2.4. X-ray powder diffractometry

X-ray powder diffraction patterns were collected with a Philips PW 1130 powder diffractometer (Co Kα radiation), over the 10–50 2Θ range at a scan rate of 1° per minute.

2.5. Scanning electron microscopy

SEM photographs were recorded on a Philips XL-30 scanning electron microscope. Prior to examination, samples were gold sputter-coated to render them electrically conductive (fine coat ion sputter JFC-1100 JEOL). Magnification selected was 2600×.

2.6. Dissolution rate studies

In vitro dissolution rate studies of the pure drug and the different drug–polymer combinations were performed according to the dispersed amount method (Nogami et al., 1969). Freshly sieved (75–150 μm) solid systems containing 30 mg of drug were added to 75 ml of water at 37 ± 0.5 °C and stirred at 100 rpm. At time intervals, samples were withdrawn with a syringe filter (pore size 0.45 μm) and spectrometrically

assayed (Perkin-Elmer Mod. 552S) for drug content. A correction was calculated for the cumulative dilution caused by replacement of the sample with an equal volume of original medium. Each test was repeated four times (coefficient of variation C.V. < 1.5%). Dissolution efficiency (D.E.) was calculated from the area under the dissolution curve at time t and expressed as a percentage of the area of the rectangle described by 100% dissolution in the same time (Khan, 1975).

2.7. Cell cultures

The Caco-2 cell line was kindly provided by Dr. A. Zweibaum and Dr. M. Rousset (INSERM U170, Villejuif, France). Cells were grown routinely in T-flasks at 37 °C in a 10% CO_2/90% air atmosphere. The culture medium consisted of Dulbecco's modified Eagle's medium (DMEM, pH 7.4) containing 10% fetal bovine serum (FBS) and 1% non-essential amino acids (NEAA) (Life Technologies Eragny, France). All cells used in these studies were received at passage 8 and used at passages 80–85. The cells were seeded at a density of 10^2 cells/cm^2 on tissue culture-treated polycarbonate filters (area 1.13 cm^2) in Costar Snapwell six-well plates (Costar Europe Ltd., Badhoevedorp, Netherlands). The culture medium, added with 110 IU/ml benzylpenicillin G and 100 μg/ml streptomycin sulphate (Life Technologies Eragny) was changed every second day and cell cultures were kept at a temperature of 37 °C in an atmosphere of 95% relative humidity, 10% CO_2. Filters were used for transport studies 21–28 days after seeding (Kotzé et al., 1997).

2.8. Transport studies

Test solutions were prepared by dissolving, under magnetic stirring, 2.5 mg of NAP (as such or as 30/70 or 10/90, w/w, physical or coground mixture with CS base or its salts) in 100 ml of pH 7-buffered Hanks' balanced salt solution (HBSS) thermostated at 37 °C.

For the dynamic transport experiments, filters were placed into Grass-Swettana chambers, thermostated at 37 °C, in the presence of 1.5 ml pH 7-buffered HBSS on both the sides of the chambers, in an atmosphere of 95% air and 5% CO_2. After equilibration of the system, 1.5 ml of test solution were added to the apical side of the cells (total volume 3 ml). At given time intervals (5, 30, 60 and 120 min), samples (200 μl) withdrawn from the basolateral side, replaced with an equal volume of fresh HBSS solution, were assayed for drug content by HPLC, as described in Section 2.10. Results were corrected for dilution and expressed as cumulative transport as a function of time. Each experiment was performed on six filters contemporaneously.

The apparent permeability coefficient was calculated by the following equation:

$$P_{app} = \frac{dQ}{dt}\frac{1}{A}\frac{1}{C_o}$$

where P_{app} is the apparent permeability coefficient (cm/s), dQ/dt (μg/s) is the rate of appearance of the drug on the basolateral side, A is the surface area of the monolayers (1.13 cm^2), and C_o (μg/ml) is the initial drug concentration in the donor compartment.

A mass balance calculation was also performed to determine if accumulation or metabolism of the solute or adsorption to the apparatus occurred (Pade and Stavchansky, 1997). One-way analysis of variance (ANOVA) followed by the Student–Newman–Keuls multiple comparison test (Graph Pad Prism, Version 3) was used to compare the observed differences.

2.9. Measurement of the trans-epithelial electrical resistance (TEER)

The values of TEER were determined by measuring the potential difference between the two sides of the cell monolayer using a Millicell® ERS meter (Millipore, Bedford, MA, USA) connected to a pair of chopstick electrodes (Borchard et al., 1996). Measurements started 10 min prior to incubation on the apical size of the cells with the testing and blank solutions. All experiments were performed in sextuple in a 95% air and 5% CO_2 atmosphere at 37 °C. Average TEER values for untreated cell monolayers were over 350.

Lucifer Yellow (St. Quentin Fallavier, France), a hydrophilic fluorescent dye, was used to check the junction integrity of Caco-2 cells during the experiments. 300 μl of a HBSS solution of Lucifer Yellow (3 mg/100 ml) were added to the apical side and, at time intervals (5, 30, 60 and 120 min), samples were withdrawn from the basolateral side and assayed using a fluorescence 96-well plate reader Cytofluor™

4000 (Perkin-Elmer). Results were corrected for dilution and expressed as cumulative transport at time *t*.

2.10. High performance liquid chromatography (HPLC) assay

HPLC analyses were performed with a Shimadzu SPD-6A apparatus equipped with an injector valve with a 20 μl sample loop (Mod. Rheodyne) using a Luna C18 (5 μm 150 mm × 4.6 mm i.d., Phenomenex®) column. The mobile phase consisted of a mixture of 0.02 M phosphate buffer (adjusted at pH 3 with 96%, v/v, phosphoric acid), acetonitrile, and methanol (40:10:50, v/v). The flow rate was 1 ml/min and NAP was detected spectrometrically (Shimadsu LC-6A) at 280 nm. Linearity ($r^2 > 0.995$) was checked in the 0.3–18 μg/ml concentration range. No interference has been found for the marker Lucifer Yellow.

3. Results and discussion

3.1. Dissolution studies

The results of dissolution studies performed on 30/70 (w/w) drug–polymer physical mixtures and coground products are shown in Fig. 1 and summarized in Table 1 in terms of dissolution efficiency and percent of drug dissolved at 60 min. The relative dissolution rate at 5 min, in comparison to the drug alone, and the pH value of each solution are also reported. It is evident that all chitosan types increased NAP dissolution rate and dissolution efficiency with respect to pure drug, but the base form CS was the most effective. As for the type of chitosan salts, glutamates were more efficacious than the hydrochloride

Table 1
Dissolution efficiency (D.E. 60) and percent dissolved (P.D. 60) at 60 min of naproxen (NAP) or its 30/70 (w/w) physical (P.M.) or coground (GR) mixtures with chitosan base (CS) or glutamate (CSG113 and CSG213) or hydrochloride (CSCl113 and CSCl213) salts with the relative increment (R.I.) in comparison with pure drug, the relative dissolution rate (r.d.r.) at 5 min and the pH of their aqueous solutions

Sample	D.E. 60	R.I.	P.D. 60	R.I.	r.d.r.	pH
NAP	6.22	–	7.38	–	–	4.5
P.M. NAP–CS	14.6	2.34	16.4	2.22	3.1	5.6
GR NAP–CS	32.0	5.14	36.5	4.95	6.6	5.6
P.M. NAP–CSG113	12.7	2.04	14.8	2.00	2.5	4.8
GR NAP–CSG113	25.1	4.03	27.7	2.00	5.5	4.8
P.M. NAP–CSG213	11.6	1.86	13.5	3.75	2.2	4.8
GR NAP–CSG213	18.9	3.04	20.9	2.83	3.9	4.8
P.M. NAP–CSCl113	10.6	1.70	12.5	1.69	1.8	4.5
GR NAP–CSCl113	17.4	2.80	20.0	2.71	3.5	4.5
P.M. NAP–CSCl213	8.85	1.42	10.8	1.46	1.4	4.5
GR NAP–CSCl213	13.7	2.20	15.7	2.13	2.9	4.5

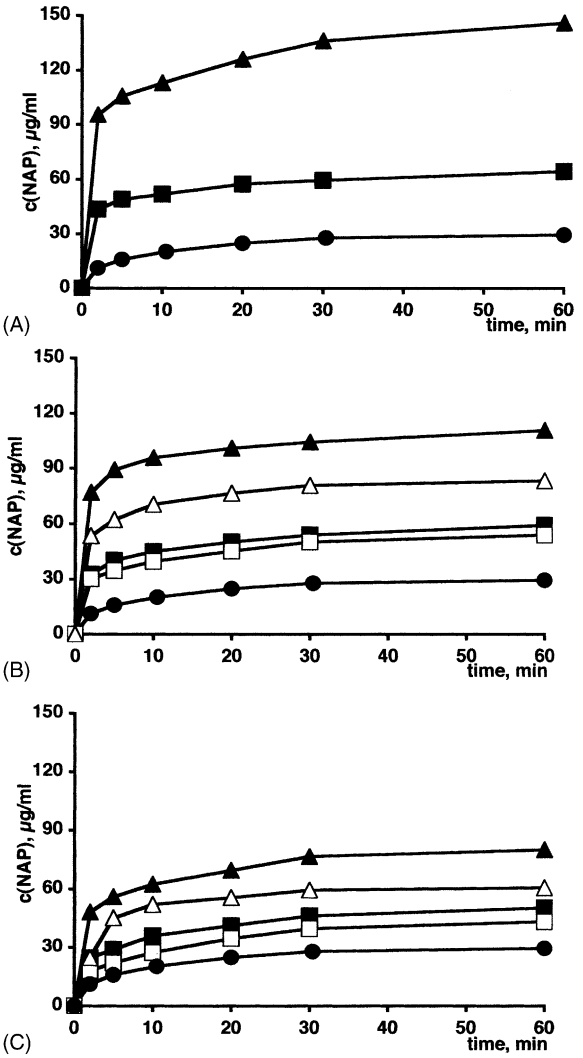

Fig. 1. Dissolution curves of naproxen (NAP) alone (●) and from 30/70 w/w physical mixtures (■, □), and coground (▲, △) products with chitosan glutamate (B) or chitosan hydrochloride (C) (for chitosan salts, black and white symbols indicate the 113 and 213 series, respectively) ($n = 4$, coefficient of variation <1.5%).

ones. The slightly higher pH of glutamate compared to hydrochloride solutions (4.8 instead of 4.45) was probably not enough to explain this effect, which is also reasonably due to a better powder wettability. For both salts, the 213 series was less effective than the corresponding 113 one, probably due to its higher molecular weight and then to the higher viscosity of its aqueous solutions leading to a lowering of drug diffusion rate. These results were consistent with previous findings that showed an inverse relationship between chitosan molecular weight and drug dissolution improvement (Mura et al., 2003; Portero

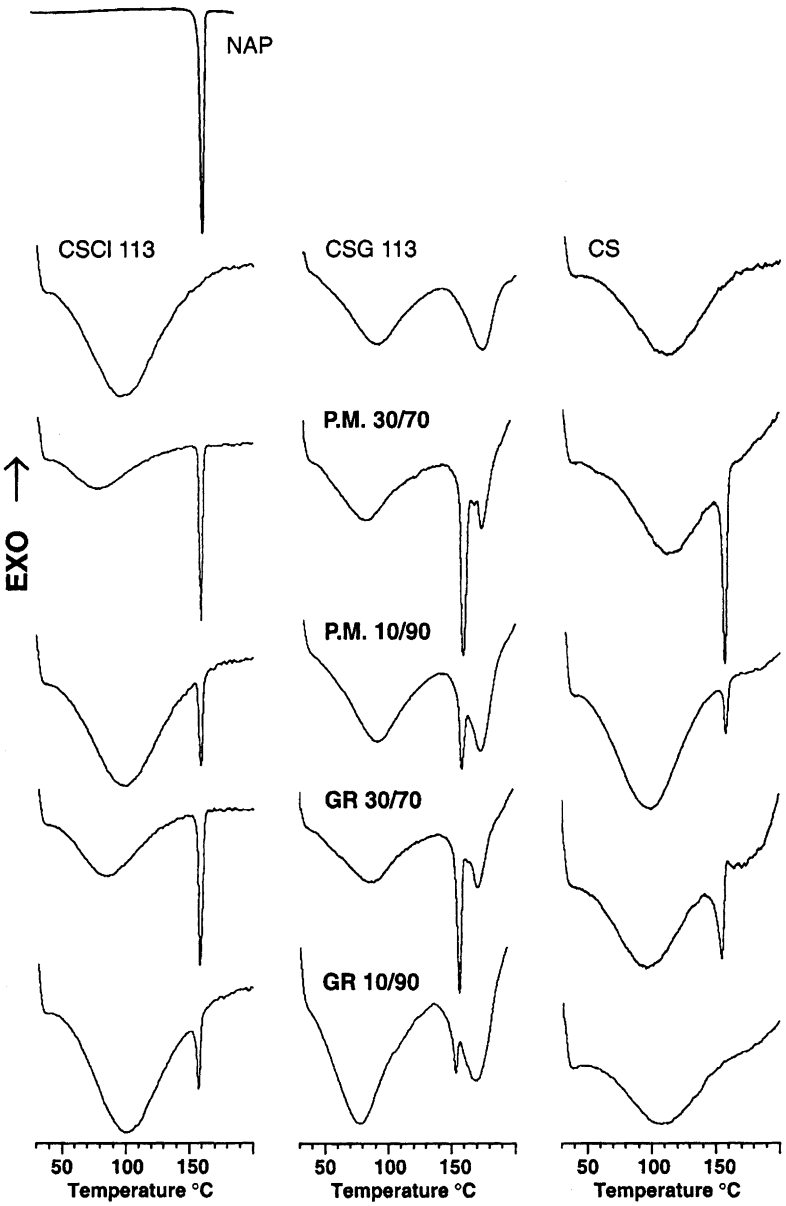

Fig. 2. DSC curves of pure naproxen (NAP), chitosan hydrochloride (CSCl113), glutamate (CSG113) and base (CS), and of drug–polymer physical (P.M.) or coground (GR) mixtures at 30/70 and 10/90 (w/w) drug-to-carrier ratios.

et al., 1998). The slight positive effect on drug dissolution rate shown by simple physical mixtures could be explained by a reduction of the interfacial tension between the hydrophobic drug particles and the dissolution medium, owing to the presence of the hydrophilic polymer. The better performance of coground products in comparison with the corresponding physical mixtures could be attributed to a decrease in drug crystallinity during cogrinding with the amorphous carrier, as well as to the particle size reduction and the better dispersion and more intimate contact between the components brought about by the mechanical treatment (Mura et al., 2003).

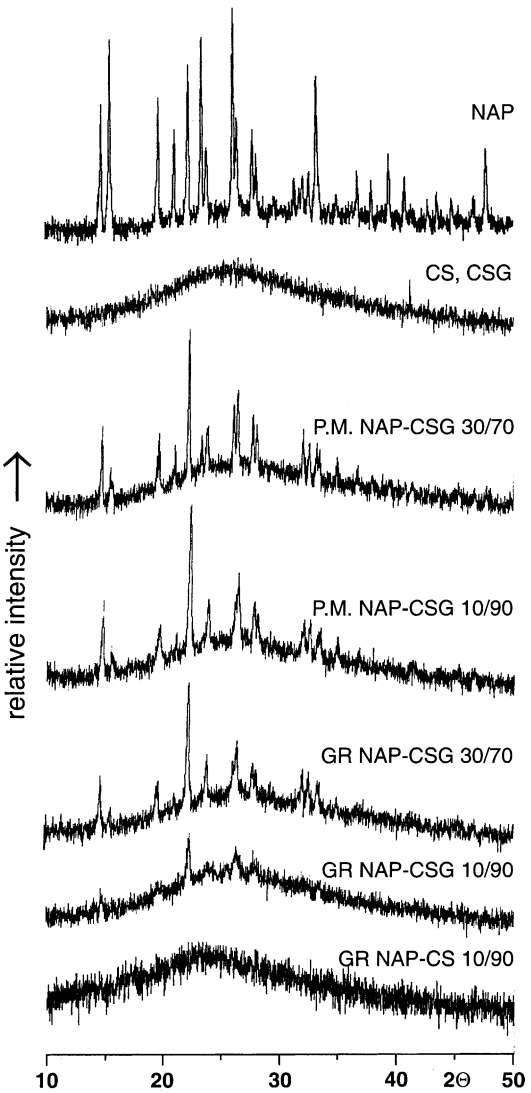

Fig. 3. X-ray powder diffraction patterns of pure naproxen (NAP), chitosan base (CS), chitosan glutamate (CSG) and 30/70 or 10/90 (w/w) drug-carrier physical (P.M.) and coground (GR) mixtures.

3.2. Solid state studies

The thermal curves of pure components and the 30/70 and 10/90 (w/w) drug–polymer physical and coground mixtures are collected in Fig. 2. The DSC curve of NAP was typical of a crystalline anhydrous substance, showing a sharp endothermal peak (T_{onset} = 153.4 ± 0.3 °C, T_{peak} = 156.7 ± 0.4 °C, fusion enthalpy 140 ± 6 J/g, four runs), corresponding to the drug melting. The DSC profiles of CS and both its salts, typical of amorphous hydrated compounds, exhibited a broad endothermal effect between 50 and 130 °C, due to their dehydration process. Chitosan glutamate showed an additional broad endothermal effect between 150 and 180 °C, typical of this polymer, as also observed by other authors (Portero et al., 1998; Genta et al., 2003). The characteristic thermal profile of the drug was clearly detectable in all the physical mixtures, even though a progressive size reduction of its endothermal peak, with a concomitant lowering of the onset temperature, was observed with increasing polymer content. This effect, which is directly related to the loss of NAP crystallinity, became more marked in coground systems, due to the particle size reduction and the more intimate and homogeneous dispersion of the drug into the amorphous polymeric matrix obtained through the mechanical treatment. CS base showed the highest amorphizing

Table 2
Effects of chitosan base (CS) or as glutamate salt (CSG) on naproxen (NAP) apparent permeability (P_{app}) across Caco-2 cells

	Sample	$P_{app} \times 10^{-5}$ (cm/s)[a]
NAP		4.88 ± 0.80
NAP–CS	30/70 (w/w) physical mixture	4.50 ± 0.32
NAP–CS	30/70 (w/w) coground	4.61 ± 0.52
NAP–CSG113	30/70 (w/w) physical mixture	4.75 ± 0.57
NAP–CSG113	30/70 (w/w) coground	5.94 ± 0.59[b]
NAP–CSG113	10/90 (w/w) coground	5.95 ± 0.30[b]

[a] Mean ± S.D. ($n = 6$).
[b] Significantly different ($P < 0.01$) from all other treatments (ANOVA, Student–Newmann–Keuls multiple comparison test).

power toward NAP, probably as a consequence of more intense drug–polymer interactions in the solid state. In fact, the complete disappearance of the drug endothermal peak, indicating its complete amorphization, was observed only in the 10/90 (w/w) coground product of NAP with CS base.

Representative X-ray powder diffraction patterns of pure components and their physical and coground mixtures are shown in Fig. 3. The typical diffraction peaks of NAP were still well detectable in the respective physical mixtures with all the polymers, emerging on the diffuse background of the amorphous carrier. The loss of drug crystallinity was more evident in coground mixtures, probably as a consequence of loosening of crystal forces of NAP finely dispersed within the amorphous polymer. The amorphization phenomenon became gradually more pronounced with increasing carrier amount in the system, up to

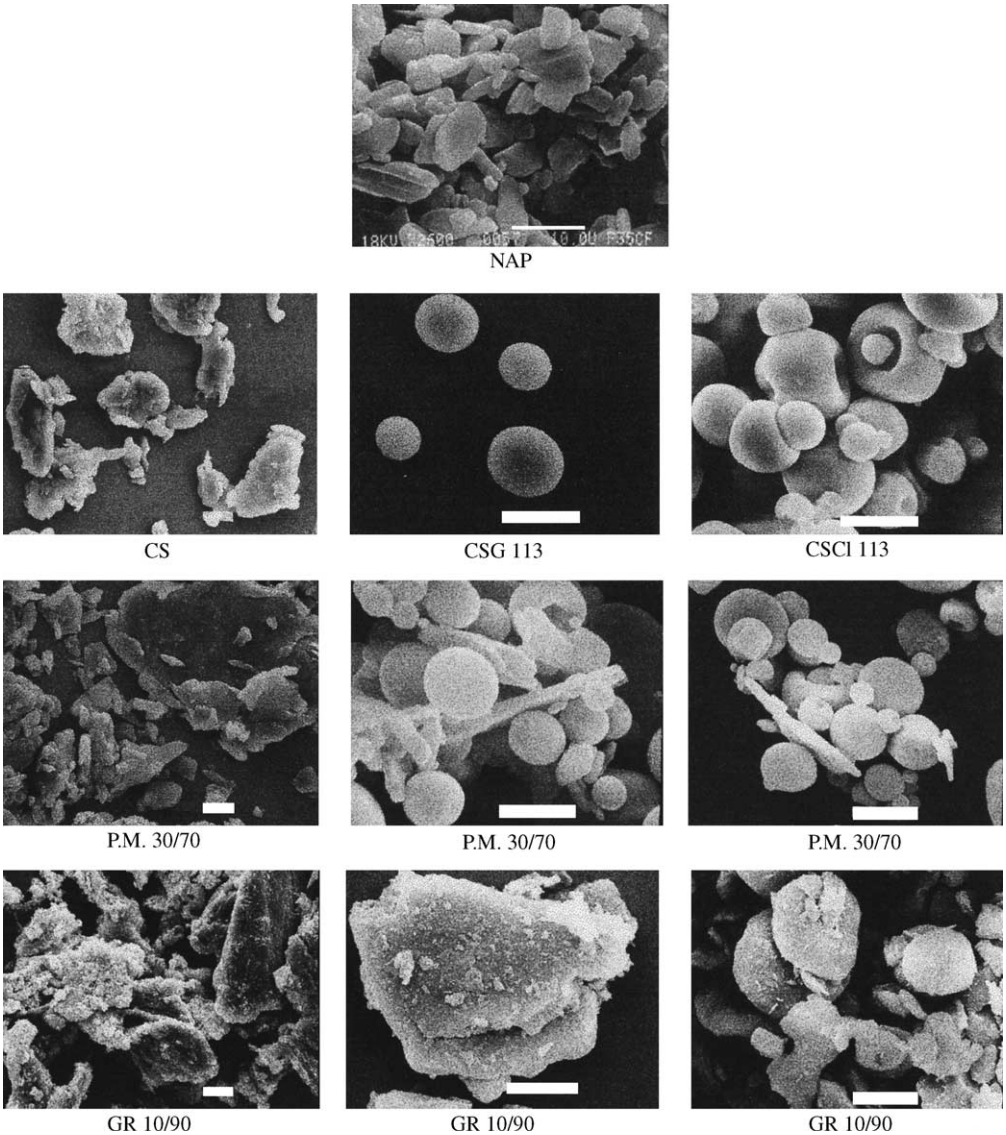

Fig. 4. SEM micrographs of pure naproxen (NAP), chitosan base (CS), chitosan glutamate (CSG113), chitosan hydrochloride (CSCl113) and 30/70 (w/w) drug-carrier physical (P.M.) and coground (OR) mixtures. The 10 μm calibration bars are shown.

complete disappearance of NAP diffraction peaks at 10/90 (w/w) NAP–CS combination. These results were in agreement with DSC findings and allowed exclusion of a possible effect of drug amorphization due to the thermal energy supplied during the DSC scan.

The morphology of the NAP–polymer systems was investigated by means of SEM analysis (Fig. 4). Drug particles appeared as small plate-like crystals (5–10 μm) with smooth surfaces of homogeneous morphology, CS consisted of amorphous particles of rather irregular size and shape, whereas CSG and CSCl particles were of typical spherical form. Crystals of NAP mixed with carrier particles were clearly evident in drug–polymer physical mixtures, whereas both drug amorphization and particle size reduction, produced by the shear and impact stresses during the high-energy cogrinding treatment, were evident in coground products, and particularly in combinations with CS base. This is probably due to the irregular surface of its amorphous particles, which evidently, favours strong solid-state interactions with the crystalline drug particles during the mechanical treatment, differently from the spherically shaped particles of chitosan salts (see Fig. 4).

In summary, all solid state studies indicated that CS base exhibited a more marked drug amorphization power than its salts. Therefore, such results seem to confirm the importance of the drug amorphization process in the improvement of its dissolution properties, pointing out a possible relationship between the solubilizing efficiency and the amorphizing power toward NAP of the examined chitosans.

3.3. Transport studies

On the basis of the dissolution study results, and in order to evaluate the effect of both chitosan type (base or glutamate salt), polymer content in the product (70 or 90%, w/w) and sample preparation method (simple physical mixing or high-energy cogrinding) on NAP permeability across Caco-2 cells monolayers, 30/70 (w/w) NAP–CS and NAP–CSG113 physical mixtures and coground products and NAP–CSG113 10/90 (w/w) coground system were selected for transport studies. The transport of NAP alone was also tested as control.

The permeation profiles of NAP from the different tested samples are depicted in Fig. 5. The apparent permeability coefficients (P_{app}) calculated from the linear portion of permeation profiles (30–120 min), are shown in Table 2. The P_{app} value obtained for NAP alone was consistent with the one reported by Pade and Stavchansky (1998) in a static transport study ($3.9 \pm 0.3 \times 10^{-5}$ cm/s). The slightly higher value

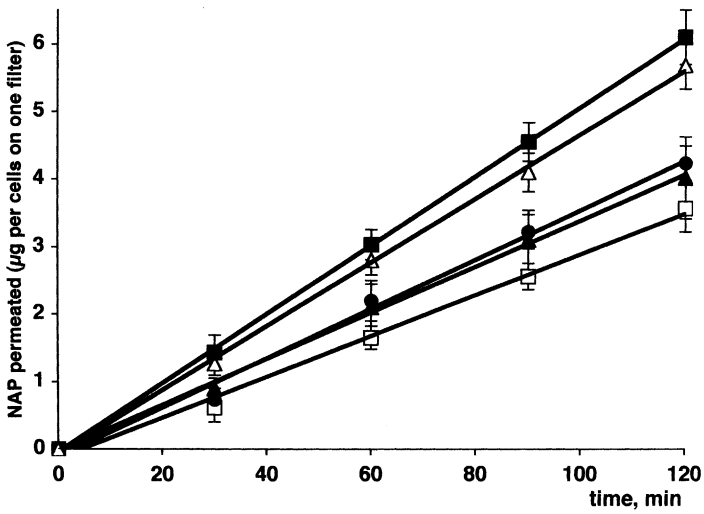

Fig. 5. Permeation profiles of naproxen alone and from its physical (P.M.) and coground (GR) mixtures with chitosan base (CS) and chitosan glutamate (CSG113) across Caco-2 cell monolayers. Key: NAP alone (▲), NAP–CS GR 30/70 (w/w) (□), NAP–CSG113 P.M. 30/70 (w/w) (●), NAP–CSG113 GR 10/90 (w/w) (△), NAP–CSG113 GR 30/70 (w/w) (■). Each point represents the mean of six experiments.

found in our studies is altributable to the stirring of the medium produced by air insufflation during the dynamic transport. In fact, stirring reduces the thickness of the stationary aqueous layer that covers the monocellular layer and hinders drug permeation (Karlsson and Artursson, 1991). No significant P_{app} variation ($P > 0.05$) was found for NAP–CS binary systems with respect to NAP alone, whereas, on the contrary, the values obtained for 30/70 and 10/90 (w/w) NAP–CSG113 coground mixtures were significantly higher ($P < 0.01$).

TEER variation and Lucifer Yellow flux recorded during the transport experiments are reported in Fig. 6. Measurements of the TEER were performed in order to verify the tightness of the junctions between cells (Borchard et al., 1996) and as an aid in interpreting the results of drug permeation studies. No cellular damage occurred during the experiments

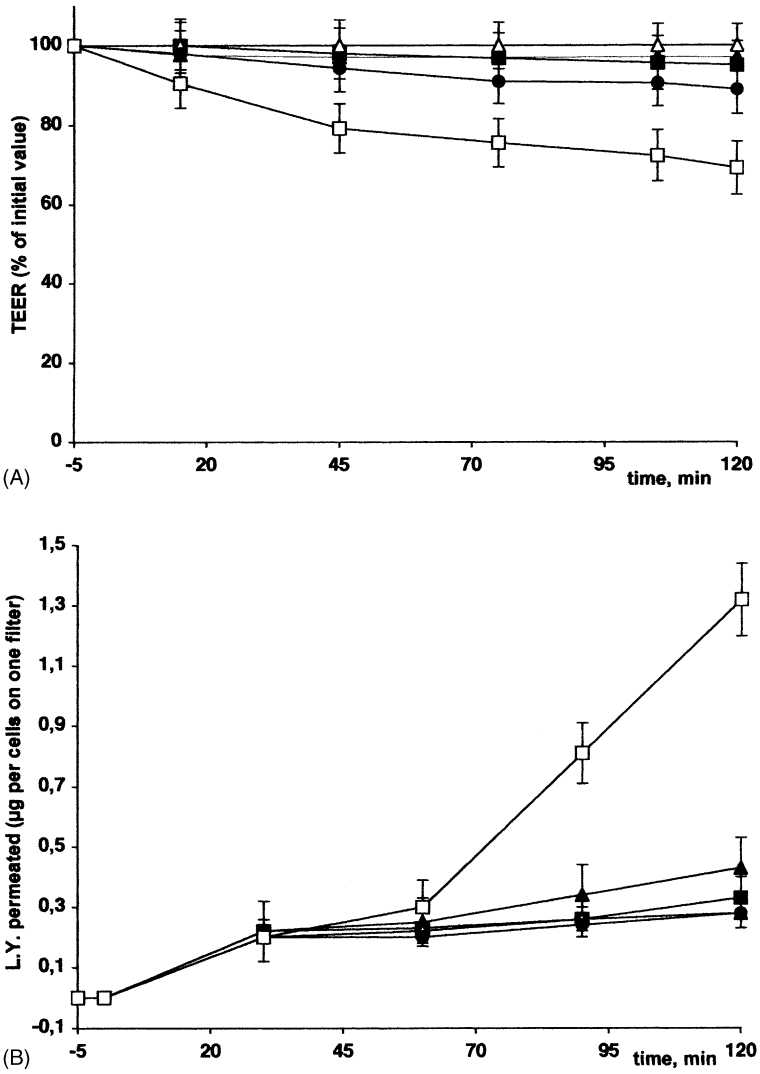

Fig. 6. TEER variation (graph A) and Yellow Lucifer flux across the Caco-2 cell monolayers (graph B) during the transport experiment in the presence of naproxen alone or its physical (P.M.) and coground (GR) mixtures with chitosan base (CS) and chitosan glutamate (CSG113). Key: NAP alone (▲), NAP–CS GR 30/70 (w/w) (□), NAP–CSG113 P.M. 30/70 (w/w) (●), NAP–CSG113 GR 10/90 (w/w) (△), NAP–CSG113 GR 30/70 (w/w) (■). Each point represents the mean of six experiments.

since the TEER variation was never higher than 40%. CS was able to both decrease the TEER of Caco-2 monolayers and increase the hydrophilic marker permeability ($P < 0.05$), probably as a consequence of tight junction opening (Illum, 1998). This effect appeared evident after about 45–60 min after sample addition to the apical side of the cells, the time necessary to induce cellular modification. However, transport studies showed that CS was unable to increase drug permeability. These findings seem to confirm that NAP permeation prevalently occurred by transcellular pathway (Pade and Stavchansky, 1998) and not through the paracellular route. Therefore, the improvement of NAP analgesic action and reduction of its effective dose obtained in in vivo experiments in mice after oral drug administration as coground with CS (Zerrouk et al., 2004) have to be mainly attributed, in addition to the polymer solubilizing effect, to its excellent mucoadhesive properties (Illum, 1998; Paul and Sharma, 2000) that allowed longer permanence times of drug in the absorption site, thus giving rise to higher drug absorption. In contrast, all CSG113 combinations were ineffective, at the concentrations used, in opening epithelial tight junctions, as demonstrated by unchanged TEER and lack of enhancer effect of the marker flux ($P > 0.05$). On the other hand, unexpectedly, transport studies showed that both CSG113 coground mixtures increased NAP permeability ($P < 0.01$). Since the corresponding physical mixtures were ineffective, this effect could probably be explained by the formation, during the cogrinding process of NAP with this particular polymer in the high-energy vibrational micromill, of an “activated”, more permeable form. However, further in-depth investigations will be carried out to confirm this preliminary hypothesis.

4. Conclusion

All the examined chitosans were effective in improving NAP dissolution rate. CS base, in spite of its lower water solubility, showed better solubilizing properties than its salts, probably related to its stronger amorphizing power towards the drug, as emerged from solid state studies. Polymers at low molecular weight exhibited better performance than the corresponding ones at higher molecular weight, probably due to the lower viscosity of their aqueous solutions. Mechano-chemical activation in a high-energy mill of drug–polymer combinations was always more efficacious in improving drug dissolution than simple mixing.

Transport studies showed that coground systems with CS base significantly ($P < 0.05$) decreased the TEER of Caco-2 cells and increased the hydrophilic marker permeability, but did not cause significant variations of the drug apparent permeability. On the contrary, drug–CSG113 coground systems, at the same concentration, did not have any effect on the opening of epithelial tight junctions of Caco-2 cells (as demonstrated by unchanged TEER values), whereas allowed a significant ($P < 0.01$) improvement of NAP apparent permeability.

It is evident that further studies will be necessary to better investigate the enhancer absorption properties of CSG113 towards NAP. However, from these preliminary results, it can be concluded that NAP–CSG113 coground mixure seems to be the most powerful system, among those examined, for the realization of an efficacious NAP oral formulation. In fact, it emerged as the best compromise between drug dissolution enhancement and permeation improvement, without interfering with the epithelial intestinal barrier functionality.

Acknowledgements

Lai Kuen Renè is gratefully acknowledged for his help in performing scanning electron microscopy analyses. Financial support from MURST is acknowledged.

References

Açikgoz, M., Kas, H.S., Hasçelik, Z., Milli, U., Hincal, A.A., 1995. Chitosan microspheres of diclophenac sodium, II: in vitro and in vivo evaluation. Pharmazie 50, 275–277.

Amidon, G.L., Lennernäs, H., Shah, V.P., Crison, J.R., 1995. A theoretical basis for a biopharmaceutic drug classification: the correlation of in vitro drug product dissolution and in vivo bioavailability. Pharm. Res. 12, 413–420.

Artursson, P., 1991. Cell culture as models for drug absorption across the intestinal mucosa. Crit. Rev. Ther. Drug Carrier Syst. 8, 105–130.

Artursson, P., Lindinark, T., Davis, S.S., Illum, L., 1994. Effect of chitosan on permeability of monolayer of intestinal epithelial cells (Caco-2). Pharm. Res. 11, 1358–1361.

Baldrick, P., 2000. Pharmaceutical excipient development: the need for preclinical guidance. Regul. Tox. Pharmacol. 32, 210–218.

Borchard, G., Lueßen, H.L., de Boer, A.G., Verhoef, J.C., Lehr, C., Junginger, H.E., 1996. The potential of mucoadhesive polymer in enhancing intestinal peptide drug absorption. III: effect of chitosan-glutamate and carbomer on epithelial tight junction in vitro. J. Control. Rel. 39, 131–138.

Dodane, V., Amin Khan, M., Merwin, J.R., 1999. Effect of chitosan on epithelial permeability and structure. Int. J. Pharm. 182, 21–32.

Genta, I., Perugini, P., Modena, T., Pavanetto, F., Castelli, F., Muzzarelli, R.A.A., Muzzarelli, C., Conti, B., 2003. Miconazole-loaded 6-oxychitin-chitosan microcapsules, Carbohydrate. Polymer 52, 11–18.

Illum, L., 1998. Chitosan and its use as a pharmaceutical excipient. Pharm. Res. 15, 1326–1331.

Karlsson, J., Artursson, P., 1991. A method for the determination of cellular permeability coefficients and aqueous boundary layer thickness in monolayers of intestinal epithelial (Caco-2) cells grown in permeable filter chambers. Int. J. Pharm. 71, 55–64.

Khan, K.A., 1975. The concept of dissolution efficiency. J. Pharm. Pharm. 27, 48–49.

Kotzé, A.F., de Leeuw, B.J., Lueßen, H.L., de Boer, A.G., Verhoef, J.C., Junginger, H.E., 1997. Chitosans for enhanced delivery of therapeutics peptides across intestinal epithelia: in vitro evaluation in Caco-2 cell monolayers. Int. J. Pharm. 159, 243–253.

Lennernäs, H., Palm, K., Fagerholm, U., Artusson, P., 1996. Comparison between active and passive drug transport in human intestinal epithelial (Caco-2) cells in vitro and human jejunum in vivo. Int. J. Pharm. 127, 103–107.

Mura, P., Zerrouk, N., Mennini, N., Maestrelli, F., Chemtob, C., 2003. Development and characterization of naproxen-chitosan solid system with improved drug dissolution properties. Eur. J. Pharm. Sci. 19, 67–75.

Niazi, S.K., Alam, S.M., Alirnad, S.I., 1996. Dose dependent pharmacokinetics of naproxen in man. Biopharm. Drug Dispos. 17, 355–361.

Nogami, H., Nagai, T., Yotsuyanagi, I., 1969. Dissolution phenomena of organic medicinals involving simultaneous plasse changes. Chem. Pharm. Bull. 17, 499–509.

Pade, V., Stavchansky, S., 1997. Estimation of the relative contribution of the transcellular and paracellular pathway to the transport of passively absorbed drugs in the Caco-2 cell culture model. Pharm. Res. 14, 1210–1215.

Pade, V., Stavchansky, S., 1998. Link between drug absorption solubility and permeability measurements in Caco-2 cells. J. Pharm. Sci. 87, 1604–1607.

Paul, W., Sharma, C.P., 2000. Chitosan, a drug carrier for the 21st century. S.T.P. Pharma Sci. 10, 5–22.

Portero, A., Remuñan-Lopez, C., Vila-Jato, J.L., 1998. Effect of chitosan and chitosan glutamate enhancing the dissolution properties of the poorly water soluble drug nifedipine. Int. J. Pharm. 175, 75–84.

Schipper, N.G.M., Varum, K., Stenberg, M.P., Ocklind, G., Lennernäs, H., Artursson, P., 1999. Chitosan as absorption enhancers for poorly absorbable drugs: 3: influence of mucus on absorption enhancement. Eur. J. Pharm. Sci. 8, 335–343.

Zerrouk, N., Mennini, N., Maestrelli, F., Chemtob, C., Mura, P., 2004. Comparison of the effect of chitosan and polyvynilpyrrolidone on dissolution properties and analgesic effect of naproxen. Eur. J. Pharm. Biopharm. 57, 93–99.